

# Near-infrared spectroscopy as a potential method for identification of anatomically similar Japanese diploxylons

Yoshiki Horikawa · Suyako Mizuno-Tazuru · Junji Sugiyama

Received: 4 November 2014 / Accepted: 5 January 2015 / Published online: 31 January 2015  
© The Japan Wood Research Society 2015

**Abstract** A reliable technique for distinguishing anatomically similar diploxylons, *Pinus densiflora* and *P. thunbergii*, was designed by employing near-infrared (NIR) spectroscopy in combination with multivariate analysis. In total, 24 wood blocks, with half of them being of *P. densiflora* and the rest of *P. thunbergii*, were selected from the collections of the Kyoto University xylarium and scrutinized to build an acceptable model for discriminating between the two species. The prediction model was constructed only from heartwood, and the best performance was obtained for wavenumbers of 7,300–4,000  $\text{cm}^{-1}$  in the second derivative spectra. To apply this model to actual materials obtained from historical wooden buildings, 12 aging wood samples were analyzed and compared by microscopic identification. Unexpectedly, the spectral differences between the species were smaller than those caused by aging, and the prediction error was approximately 50 %. The spectra of the aging samples were quite distinct in the specific region characteristic of absorbed water (5,220  $\text{cm}^{-1}$ ); this was demonstrated clearly by principal component analysis. Therefore, for the proposed model to be suitable for use in practical applications, further investigations of aging wood samples and the corresponding spectroscopic data are necessary to understand the effects of aging on the spectral data.

**Keywords** Discriminant analysis · NIR spectroscopy · Japanese diploxylons · Wood identification · Aging wood

## Introduction

*Pinus densiflora* and *P. thunbergii* are varieties of pine trees that are very popular in Japan. The former is known as akamatsu and mematsu, and the latter as kuromatsu and omatsu. Both are planted widely in Japan for timber production and as ornamental trees and are a characteristic feature of classical Japanese gardens. *P. densiflora* is commonly seen growing on the low mountains and hill-sides, while *P. thunbergii* is native to the coastal areas.

Anatomically, the two species are nearly identical in terms of the resin canal, which is surrounded by thin-walled epithelial cells and window-type cross-field pitting and exhibits a distinct transition from earlywood to latewood. The key difference between the two species was reported to be the degree of dentate thickening of the ray tracheids (Fig. 1). However, this difference is rather subjective and can be misleading, particularly in old samples, whose cell walls have nearly deteriorated. Consequently, in many previous studies, these pine wood species have been identified simply as diploxylons and their particular species has been left undecided. Therefore, an alternative method that could allow for the identification of the particular species without requiring special experimentation would be highly desirable.

In this regard, near-infrared (NIR) spectroscopy, which is known as a rapid, accurate and reproducible analysis technique, is an attractive choice. NIR spectroscopy is also suitable for assessing wood materials because the bands attributable to the vibrations of the chemical bonds involved in the formation of the cell wall allow for the direct and indirect estimation of the chemical and physical properties of the materials. When combined with multivariate analysis, NIR spectroscopy can be used to distinguish between different wood species. Schimleck et al. [1]

Y. Horikawa (✉) · S. Mizuno-Tazuru · J. Sugiyama  
Research Institute for Sustainable Humanosphere, Kyoto  
University, Uji 611-0011, Japan  
e-mail: yhorikawa@rish.kyoto-u.ac.jp

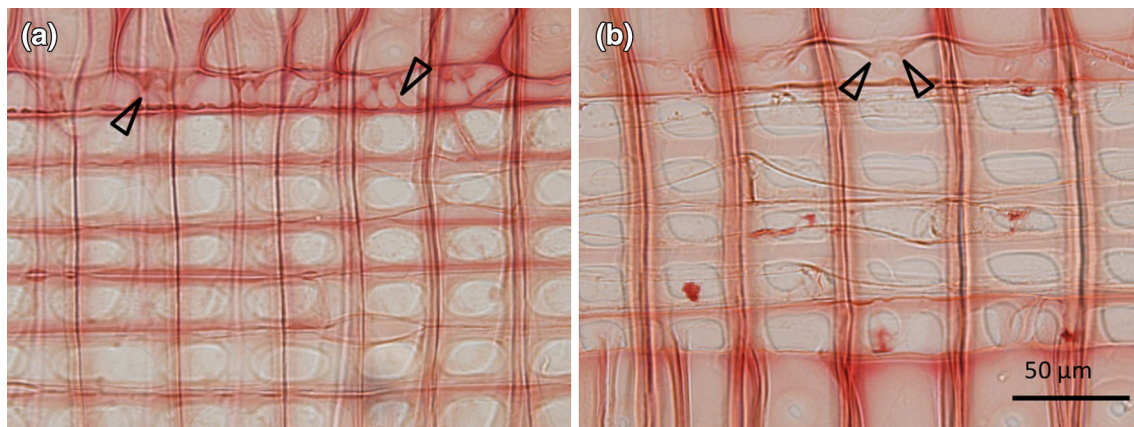


**Fig. 1** Optical micrographs of the standard radial section. **a** *P. densiflora* shows dentate thickening within the ray tracheid, while **b** these features are smooth in *P. thunbergii*. The arrow heads indicate dentate thickening

demonstrated that principal component analysis (PCA) could be used to distinguish between pine and eucalyptus and also to differentiate between samples of the same eucalyptus species grown at different sites. Soft independent modeling of class analogy has also been used to classify wood samples, including red and white oak [2] and larch species [3]. Regression analysis, especially partial least square (PLS) regression, is a powerful method of accurately estimating the chemical compositions of wood samples [4] and of determining their enzymatic hydrolysis [5] and decay resistance [6], in addition to their physical properties, such as fiber length [7–9], cellulose microfibril angle [10], and stiffness [11]. The method of distinguishing species coupled with regression analysis, called partial least squares-discriminant analysis (PLS-DA), has been used as a tool for differentiating true mahogany from three other similar species [12, 13]. Sandberg and Sterley [14] could successfully distinguish between heartwood and sapwood samples of Norway spruce using the PLS algorithm. Watanabe et al. [15] could differentiate between aging and degraded samples of softwood, such as *Chamaecyparis obtusa*, *Torreya nucifera*, and *C. pisifera* using PLS.

In this study, we first describe a simple technique that uses NIR spectroscopy in combination with PLS-DA for distinguishing *P. densiflora* from *P. thunbergii*, which were classified at the xylarium of Kyoto University. The discriminant model was initially examined using complete sets of the wood samples. Later, the sapwood and heartwood samples were analyzed separately. Next, we demonstrate the applicability of the proposed method in determining the species of aging samples of wood, and discuss the factors that influence the precision of discrimination.

## Materials and methods

### Sampling

Wood blocks of *P. densiflora* designated as KYOw00029, 00225, 08058, 08059, 09268, 13942, 19360, and 19361, and those of *P. thunbergii* designated as KYOw00030, 00520, 05509, 05639, 08071, 10321, 11386, 13913, and 19176 by the xylarium at the Research Institute for Sustainable Humanosphere, Kyoto University (<http://database.rish.kyoto-u.ac.jp/cgi-bin/bmi/en/namazu.cgi>) were used for establishing the discriminant model. The wood samples in these blocks were collected from all the sapwood and heartwood zones. However, in the case of the wood blocks of KYOw00029, 05639, 08071, 09268, and 13913, only sapwood was collected. On the other hand, only heartwood was taken from KYOw00520, 19176, 19360, and 19361. Three parts were collected randomly from each wood block after NIR spectral analysis. Finally, wood samples from Chion-In temple in Kyoto, Japan and designated as KYO\_ID\_5165, 5166, 5168, 5170, 5173, 5175, 5185, 5187, 5189, 5192, 5197, and 5252 [16] were used to test applicability of the proposed method. Blocks were collected from each of these aging samples.

### Optical microscopy

In the case of the wood samples obtained from the xylarium for the construction of the calibration model, radial sections approximately 30  $\mu\text{m}$  in thickness were cut using a sliding microtome and were stained with safranin. In the case of the wood samples from Chion-in, the corresponding sections were obtained by hand sectioning and were not stained. The sections were observed using a light

microscope (Olympus BX51) equipped with a digital camera (Olympus DP73).

NIR spectroscopy

Each wood block after air-drying was milled with a rough file to produce a powder sample. Then, a tablet was prepared by collecting approximately 0.04 g of the powder, which was hand pressed following a previously published protocol [17]. The NIR spectrum was obtained using a PerkinElmer Spectrum 100N system for wavenumbers of 10,000–4,000  $\text{cm}^{-1}$  at a spectral resolution of 16  $\text{cm}^{-1}$ ; 32

scans were made for each sample. The prepared tablet was placed directly on the NIR integrating sphere diffuse reflectance accessory (PerkinElmer), which had a triglycine sulfate detector. Both faces of each tablet were scanned. The absorbance spectrum was recorded by normalizing the single-beam spectrum against the background spectrum using a Teflon-based material (Spectralon; LabSphere, North Sutton, NH). The original spectrum was treated using the Savitzky–Golay second derivative [18] using 9 points and a fifth-order polynomial for the smoothing before the multivariate analysis.

Multivariate analysis

PLS-DA and PCA were performed using a commercial software (Unscrambler v.9.8; CAMO Software, Inc., Woodbridge, NJ). Calibration and prediction samples from the 144 spectra (72 each for the sapwood and heartwood samples) were randomly selected as the ratio at 2 to 1, that is, 96 were used for calibration, and 48 were used for the prediction set. Of the spectra used for calibration, 48 belonged to *P. densiflora* and 48 belonged to *P. thunbergii*. In the case of the spectra used for prediction, 24 belonged to *P. densiflora* and 24 belonged to *P. thunbergii*, as shown in Table 1. For the development of a discriminant model

**Table 1** The number of NIR spectra of the wood samples used for calibration and prediction

	Calibration set	Prediction set	Total
<i>P. densiflora</i>			
Sapwood	24	12	36
Heartwood	24	12	36
<i>P. thunbergii</i>			
Sapwood	24	12	36
Heartwood	24	12	36
Total	96	48	144

**Fig. 2 a** Original NIR spectra of heartwood and sapwood from *P. densiflora* and *P. thunbergii* designated as KYOw13942 and 00030, which were included in calibration set. **b** Second derivative spectra obtained from the 4 spectra in (a)

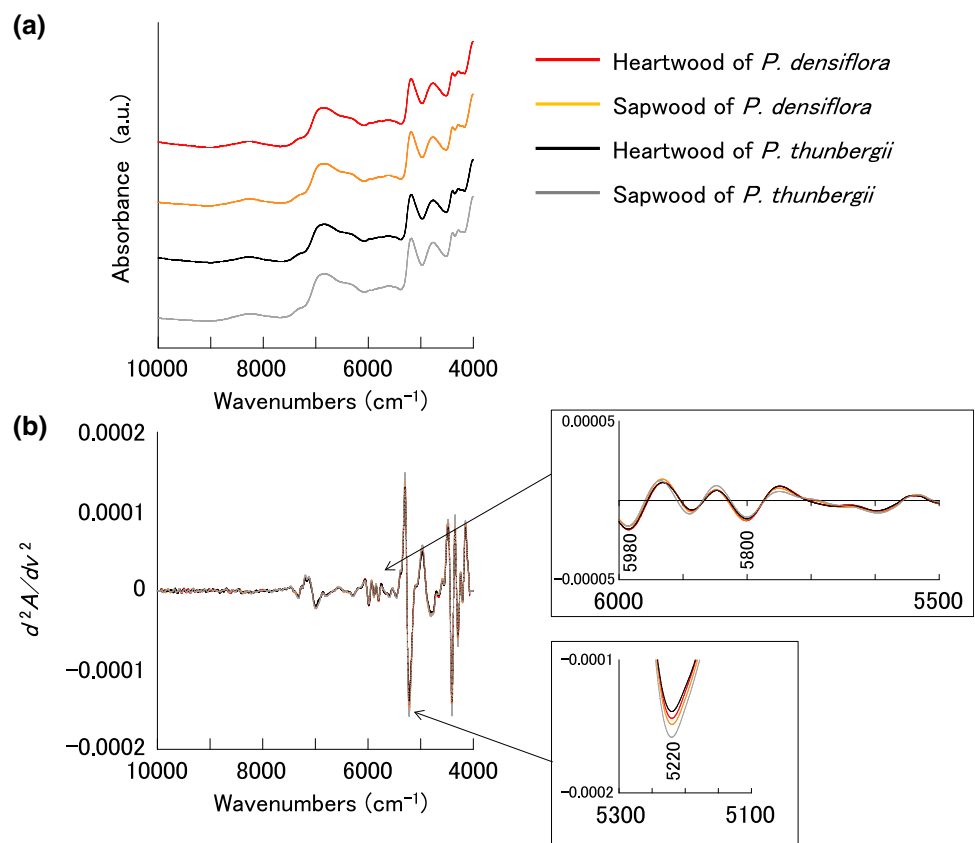


**Table 2** Statistical summary of the discriminant models based on the calibration and prediction sets obtained from a mixture of sapwood and heartwood samples (a and b), and individual sapwood (c and d) and heartwood (e and f) samples. The discriminant models were obtained by using the original spectra (a, c and e) and the second derivative spectra (b, d and f). A schematic illustration is shown on the left to indicate each spectral region

**(a)**

Spectral region ( $\text{cm}^{-1}$ )	Factors	Calibration set		Prediction set		Correct prediction (%)
		$R_c^2$	RMSEC	$R_p^2$	RMSEP	
10000 – 4000	8	0.52	0.69	0.49	0.71	93.8
7300 – 4000	10	0.66	0.58	0.58	0.65	93.8
7300 – 5500	10	0.54	0.68	0.45	0.74	85.4
6050 – 4000	10	0.65	0.59	0.57	0.66	89.6
7300 – 6050	10	0.65	0.59	0.53	0.68	91.7
5500 – 4000	10	0.65	0.59	0.53	0.68	91.7
10000 – 7300	9	0.68	0.56	0.32	0.82	79.2
7300 – 6050	7	0.32	0.82	0.25	0.87	77.1
6050 – 5500	9	0.53	0.68	0.48	0.72	83.3
5500 – 4000	9	0.61	0.62	0.56	0.66	89.6

**(b)**

Spectral region ( $\text{cm}^{-1}$ )	Factors	Calibration set		Prediction set		Correct prediction (%)
		$R_c^2$	RMSEC	$R_p^2$	RMSEP	
10000 – 4000	7	0.72	0.53	0.54	0.68	89.6
7300 – 4000	9	0.75	0.50	0.56	0.66	91.7
7300 – 5500	10	0.69	0.56	0.56	0.66	93.8
6050 – 4000	8	0.72	0.53	0.54	0.68	87.5
7300 – 6050	8	0.71	0.54	0.55	0.67	89.6
5500 – 4000	8	0.71	0.54	0.55	0.67	89.6
10000 – 7300	2	0.42	0.76	0.23	0.88	68.8
7300 – 6050	2	0.33	0.82	0.28	0.85	72.9
6050 – 5500	10	0.56	0.66	0.53	0.69	81.3
5500 – 4000	8	0.69	0.56	0.52	0.69	85.4

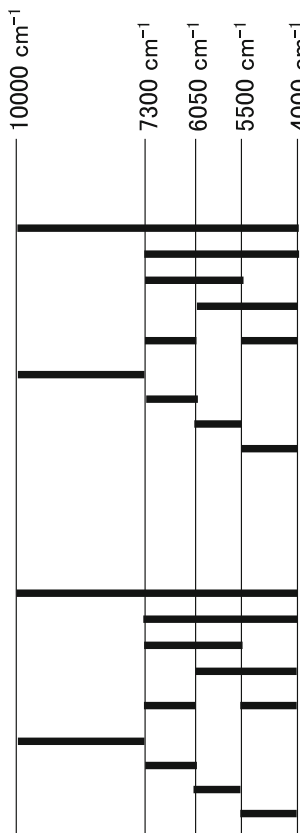
**(c)**

Spectral region ( $\text{cm}^{-1}$ )	Factors	Calibration set		Prediction set		Correct prediction (%)
		$R_c^2$	RMSEC	$R_p^2$	RMSEP	
10000 – 4000	10	0.91	0.30	0.74	0.51	91.7
7300 – 4000	9	0.90	0.31	0.69	0.56	87.5
7300 – 5500	5	0.35	0.80	0.30	0.84	75.0
6050 – 4000	10	0.90	0.32	0.64	0.60	87.5
7300 – 6050	10	0.87	0.36	0.65	0.59	87.5
5500 – 4000	10	0.87	0.36	0.65	0.59	87.5
10000 – 7300	7	0.73	0.52	0.21	0.89	83.3
7300 – 6050	6	0.33	0.82	0.01	1.07	54.2
6050 – 5500	9	0.77	0.48	0.39	0.78	79.2
5500 – 4000	10	0.86	0.38	0.60	0.63	87.5

**(d)**

Spectral region ( $\text{cm}^{-1}$ )	Factors	Calibration set		Prediction set		Correct prediction (%)
		$R_c^2$	RMSEC	$R_p^2$	RMSEP	
10000 – 4000	5	0.79	0.46	0.59	0.64	87.5
7300 – 4000	8	0.91	0.30	0.71	0.54	95.8
7300 – 5500	4	0.72	0.53	0.67	0.58	87.5
6050 – 4000	8	0.88	0.35	0.66	0.58	95.8
7300 – 6050	6	0.74	0.51	0.64	0.60	87.5
5500 – 4000	6	0.74	0.51	0.64	0.60	87.5
10000 – 7300	1	0.19	0.90	0.02	0.99	54.2
7300 – 6050	5	0.64	0.60	0.33	0.82	75.0
6050 – 5500	5	0.65	0.59	0.59	0.64	91.7
5500 – 4000	6	0.72	0.53	0.61	0.62	87.5

**Table 2** continued



(e)

Spectral region (cm <sup>-1</sup> )	Factors	Calibration set		Prediction set		Correct prediction (%)
		<i>R</i> <sub>c</sub> <sup>2</sup>	RMSEC	<i>R</i> <sub>p</sub> <sup>2</sup>	RMSEP	
10000 – 4000	9	0.92	0.28	0.80	0.45	100
7300 – 4000	9	0.93	0.27	0.75	0.50	97.9
7300 – 5500	7	0.81	0.44	0.77	0.48	100
6050 – 4000	9	0.93	0.27	0.81	0.43	100
7300 – 6050						
5500 – 4000	9	0.91	0.30	0.78	0.47	100
10000 – 7300	8	0.81	0.44	0.56	0.67	93.8
7300 – 6050	10	0.86	0.37	0.65	0.59	95.8
6050 – 5500	9	0.91	0.30	0.84	0.40	100
5500 – 4000	10	0.95	0.22	0.83	0.42	100

(f)

Spectral region (cm <sup>-1</sup> )	Factors	Calibration set		Prediction set		Correct prediction (%)
		<i>R</i> <sub>c</sub> <sup>2</sup>	RMSEC	<i>R</i> <sub>p</sub> <sup>2</sup>	RMSEP	
10000 – 4000	8	0.97	0.18	0.83	0.41	100
7300 – 4000	7	0.92	0.28	0.86	0.37	100
7300 – 5500	8	0.91	0.30	0.73	0.52	95.8
6050 – 4000	7	0.92	0.29	0.86	0.38	100
7300 – 6050						
5500 – 4000	7	0.92	0.28	0.85	0.39	100
10000 – 7300	7	0.98	0.12	0.46	0.74	75.0
7300 – 6050	5	0.82	0.43	0.48	0.72	87.5
6050 – 5500	10	0.90	0.31	0.81	0.44	100
5500 – 4000	7	0.91	0.30	0.85	0.39	100

for use in the multivariate analysis, we assigned *P. densiflora* a class value of +1 and *P. thunbergii* a class value of -1 in the calibration set. The PLS factors were determined by cross validation; a single sample was kept out of the model, and its characteristics were predicted by constructing a model without the sample. Excessively high numbers may result in overfitting; therefore, the number of PLS factors was kept at fewer than 11. The coefficient of determination for calibration (*R*<sub>c</sub><sup>2</sup>) and the root mean square error of calibration (RMSEC) were used to assess the calibration performance. The models developed were evaluated by using the coefficient of determination of prediction (*R*<sub>p</sub><sup>2</sup>) and the root mean square error of prediction (RMSEP). The percentage of correct prediction was determined as the proportion of the number of species discriminated correctly compared to the total number of samples from prediction set. PLS-DA to distinguish between sapwood and heartwood was also performed using the same procedure.

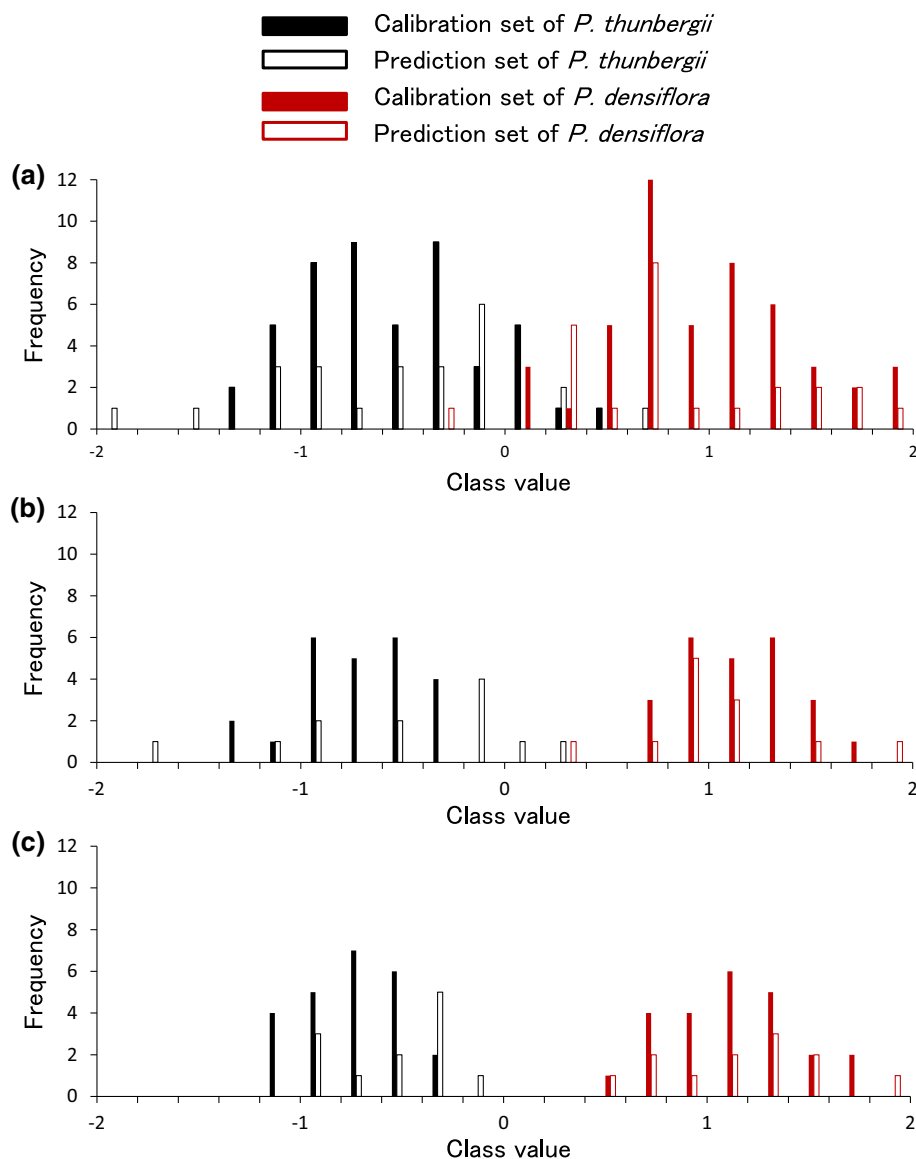
PCA was performed on the basis of the second derivative spectra of all the wood samples for wavenumbers of 7,300–4,000 cm<sup>-1</sup>. The PC loading was obtained from the model built for score plots.

**Results and discussion**

Discriminant model for determining the type of wood present

Figure 2a, b show original and second derivative spectra from heart and sapwood samples of *P. densiflora* and *P. thunbergii*. From the band at 5,220 cm<sup>-1</sup> assigned to absorbed water in second derivative NIR spectra, sapwood samples seemed higher moisture contents than those of heartwood. However, it was difficult to identify whether *P. densiflora* or *P. thunbergii* from spectra because spectral pattern including the bands at 5,980 and 5,800 specific to lignin and hemicellulose, respectively, were almost same between these species. Therefore, we applied multivariate analysis and Table 2 shows the statistical summary of the discriminant models obtained on the basis of the original spectra and the second derivative spectra. To generate a better model, the regions of the NIR spectra corresponding to the wavenumbers of 10,000–4,000 cm<sup>-1</sup> were separated into four distinct ranges on the basis of the properties of the molecular vibrations. In the first range (10,000–7,300 cm<sup>-1</sup>), the second or third overtones were involved, although less information was obtained from the

**Fig. 3** Histograms of the class values computed by PLS-DA on the basis of the second derivative spectra for wavenumbers of 7,300–4,000  $\text{cm}^{-1}$  and obtained from **a** a mixture of sapwood and heartwood, **b** sapwood, and **c** heartwood



wood samples. The second range (7,300–6,050  $\text{cm}^{-1}$ ) mainly corresponded to OH overtone vibrations. The third range (6,050–5,500  $\text{cm}^{-1}$ ) corresponded to the CH vibrations and the vibrations from the aromatic framework, while in the fourth range (5,500–4,000  $\text{cm}^{-1}$ ), several combinatorial vibrations were present.

For the samples containing both sapwood and heartwood, the discriminant models shown in Table 2a were constructed on the basis of the NIR spectra without subjecting the spectra to any spectral pretreatment. All the models were unreliable because the  $R_p^2$  values were less than 0.60. Next, we obtained the second derivative spectra and created the discriminant models shown in Table 2b. Secondary differentiation can extract information hidden in the original spectra. Thus, researchers have often applied this algorithm to construct regression models. This spectral

pretreatment decreased the number of factors relatively; however, the models obtained were not markedly better. Figure 3a shows a histogram corresponding to the discriminant model based on the second derivative spectra for 7,300–4,000  $\text{cm}^{-1}$ . In this region, a few samples of both *P. densiflora* and *P. thunbergii* had class values of approximately 0, which indicated that this model could not be used for distinguishing between the two species.

Sapwood could, therefore, be distinguished from heartwood, and discriminant models could be built, as summarized in Table 2c, d. However, as was the case with the dataset corresponding to the samples containing both sapwood and heartwood, all the models showed poor performances, as the  $R_p^2$  values were lower than 0.75. Figure 3b shows a histogram based on the second derivative spectra for 7,300–4,000  $\text{cm}^{-1}$ ; for this region, the RMSEP value

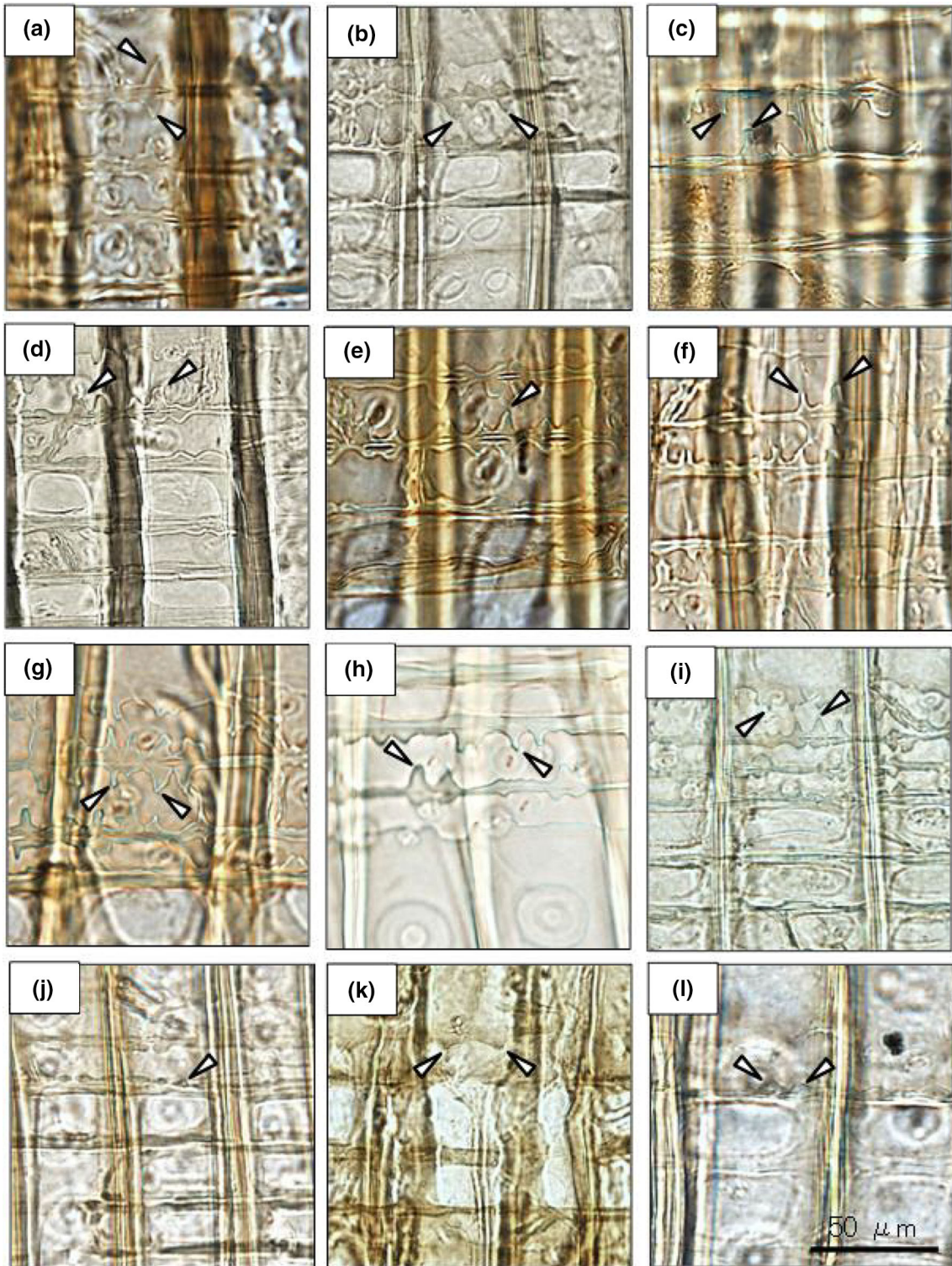
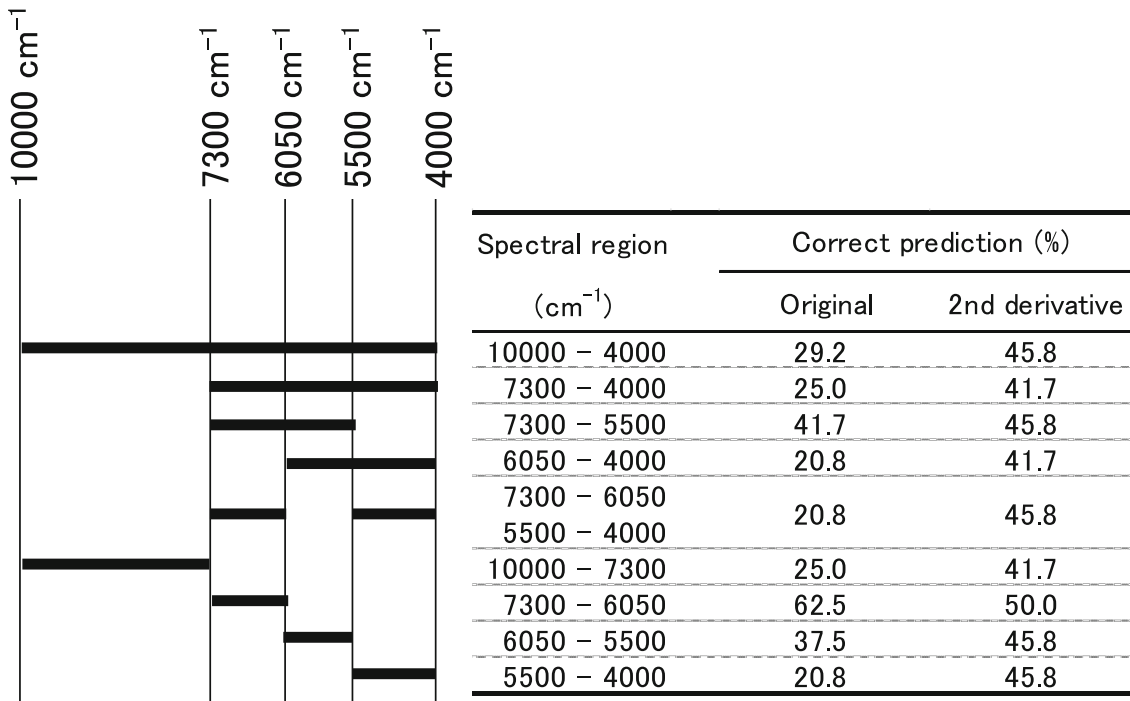


**Fig. 4** Optical micrographs of the radial sections acquired from wood samples from Chion-In temple. The images in (a)–(i) correspond to KYO\_ID\_5165, 5166, 5168, 5170, 5173, 5175, 5185, 5189, and 5252, respectively, which were identified as being of *P.*

*densiflora*. The images in (j)–(l), which were acquired from KYO\_ID\_5187, 5192, and 5197, respectively, were identified as being of *P. thunbergii*. The arrow heads indicate dentate thickening

**Table 3** Prediction accuracies of the wooden materials used in Chion-In temple as functions of the spectral pretreatment and spectral range. The predictions were made by employing the discriminant models based on the original and second derivative spectra of the heartwood sample for wavenumbers of 7,300–4,000  $\text{cm}^{-1}$ . A schematic illustration is provided on the left to show each spectral region



was 0.54 and the  $R_p^2$  value was 0.71, with some of the prediction samples from *P. thunbergii* having class values of 0 and similar to those of *P. densiflora*.

In the case of heartwood, even though a large number of factors were required, the calibration performance was comparatively better (Table 2e). However, the models obtained using the vibrations over 10,000–7,300  $\text{cm}^{-1}$  and 7,300–6,050  $\text{cm}^{-1}$  were less reliable; this was particularly true in the latter case, where the major bands were assigned to cellulose [19–21]. This suggested that the cellulose contents were indistinct between *P. densiflora* and *P. thunbergii* as well as their crystalline properties.

The discriminant models obtained using the second derivative spectra are shown in Table 2f. The models exhibited better performances as the  $R_p^2$  values corresponding to a few of the NIR spectral regions were higher than 0.85. The best performance was obtained for 7,300–4,000  $\text{cm}^{-1}$ ; this region showed an RMSEP value of 0.37,  $R_p^2$  value of 0.86 and 100 % accuracy of identification. As shown in Fig. 3c, the prediction model based on the corresponding region allowed us to classify all the samples from *P. densiflora* as having positive values, while the samples for classifying *P. thunbergii* were placed in another group and had negative values.

NIR spectroscopy is sensitive to the functional groups and is, thus, influenced by the chemical and structural features of the cell walls of the trees being investigated. Therefore, the difficulties encountered in classification using sapwood samples indicated that the chemical natures of *P. densiflora* and *P. thunbergii* were essentially indistinct. However, the fact that using heartwood samples yielded better results suggested that the heartwood components of the two species might be slightly different.

#### Applicability in investigating aging wood used in traditional buildings

The applicability of the regression model developed was tested by reexamining actual wood materials used in traditional wooden buildings built in the medieval period. Chion-In temple in Kyoto is well known and is the main temple of Jōdo Shū (“The Pure Land School”). The wood materials used in the Shūedō (i.e., the Assembly Hall) had been studied during 2005–2010, and 25 wood samples had been classified as being of diploxylons [16]. Twelve specimens were used in the present study. The enlarged radial sections of the ray tracheids of these samples are shown in Fig. 4. Of these 12 samples, only three were

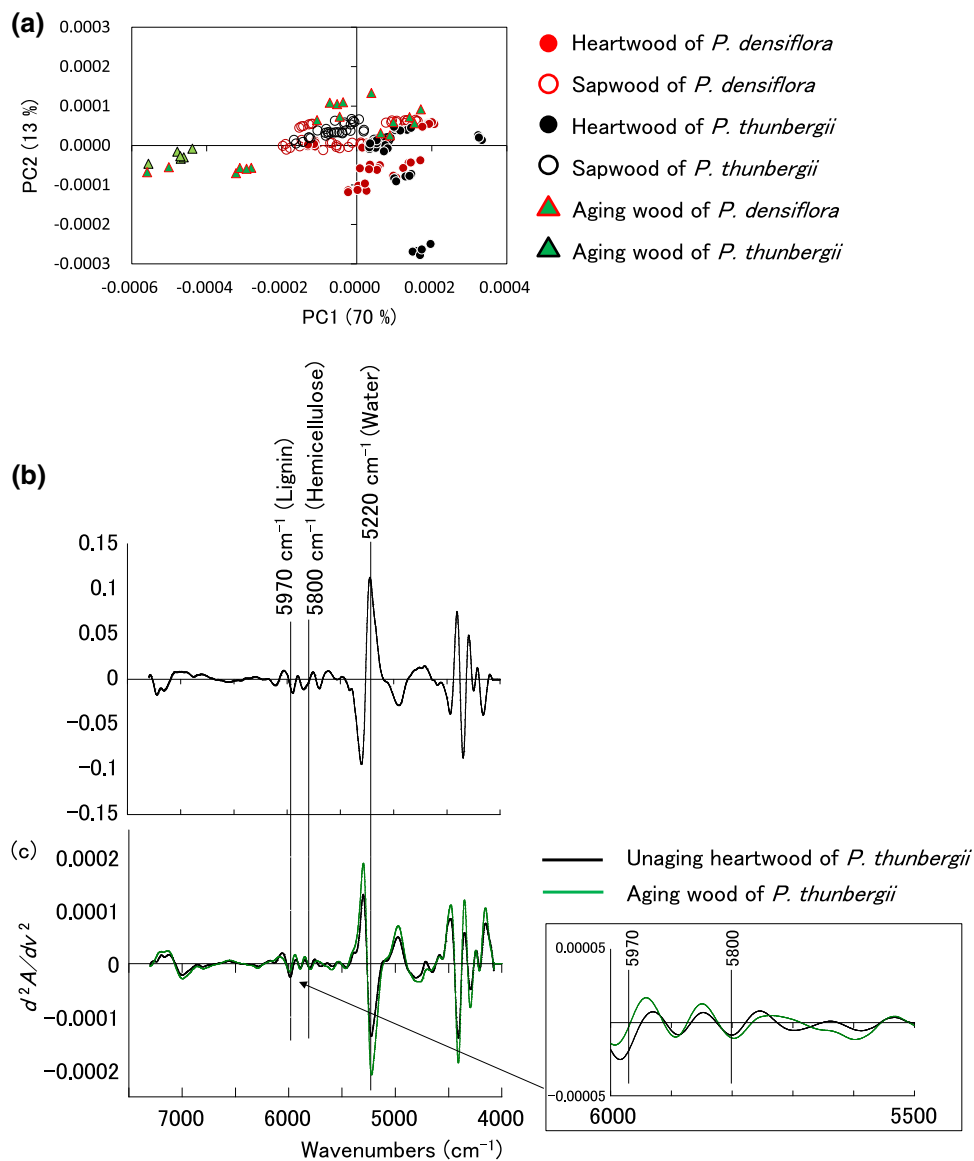


**Fig. 5** **a** The principal component analysis (PCA) scores plotted on the first and second principal components on the basis of the second derivative NIR spectra in the 7,300–4,000  $\text{cm}^{-1}$  region. **b** The spectrum obtained from PC1 loading in PCA. The bands at 5,970,

5,800, and 5,220  $\text{cm}^{-1}$  are assigned to lignin, hemicellulose, and the absorbed water, respectively. **c** Second derivative spectra obtained from unaging heartwood and aging wood of *P. thunbergii* designated as KYOw19176 and KYO\_ID\_5197

anatomically identified as *P. thunbergii* on the basis of the degree of dentate thickening in the ray tracheids. The PLS-DA models built up on the basis of heartwood were used in the identification of these materials. The percentage of coincidence with the anatomical identification results is listed in Table 3. In contrast to the prediction set samples shown in Table 2e, f, the discriminant models failed to predict the species perfectly. One possible reason behind this failure seems to be the fact that the wood used in Chion-in was sapwood, while the calibration models used for identification were created using heartwood. However, sapwood is usually not used as a building material, to

minimize deterioration and maintain the structural strength. Given this background, we investigated these aging wood samples further using NIR spectroscopy in combination with multivariate analysis, as mentioned in the next segment.

#### Effects of aging

To understand the reason for the failure in prediction of Chion-in materials, PCA was carried out in the wavenumber range 7,300–4,000  $\text{cm}^{-1}$  of the second derivative spectra (Fig. 5a). The score plots showed that some of the

wood samples from Chion-In temple localized on the left side and far from those belonging to *P. densiflora* and *P. thunbergii*. It is known that non-crystalline polysaccharides such as hemicellulose decrease in quantity in aging samples of *C. obtusa*, whereas the crystalline cellulose region is not affected [22]. Furthermore, Yokoyama et al. [23] reported that the equilibrium moisture content in *C. obtusa* decreases after aging. Therefore, it seems that aging under dry conditions degraded the hemicelluloses, which are the adsorption sites for water in wood materials, resulting in a decrease in the equilibrium moisture content. In this regard, the wood samples from Chion-in temple were different in that there was no statistical difference between modern and aging woods in hemicellulose contents, given the presence of the band at approximately  $5,800\text{ cm}^{-1}$ ; this band is specific to furanose/pyranose, which form from hemicellulose [24] and exhibited a value of almost 0 in the PC1 loading (Fig. 5b). In addition, the amount of absorbed water in the Chion-in samples was higher, as a positive band was noticed at approximately  $5,220\text{ cm}^{-1}$  and was assignable to the combinational vibration of water; this was clearly visible in the PC1 loading. Moreover, the lignin content of the Chion-in samples was lower, as a band was noticed at  $5,970\text{ cm}^{-1}$ ; this band is characteristic of aromatic skeletal vibrations [24] and exhibited negative values during PC1 loading. This interpretation was supported by the comparison with the second derivative spectra between modern and aging wood (Fig. 5c). Therefore, the lignin in the Chion-in samples seemed to be modified to a greater degree than was the hemicellulose, which resulted in a decrease in the hydrophobicity, as this increased the amount of absorbed water. These features were not observed in the spectra of the unaging wood samples. Hence, the samples from Chion-in could not be classified accurately. To be able to employ the proposed classification method for identifying historical and archeological wood samples, we have to consider the effects of aging on the characteristics of the samples, including on the quantity of absorbed water and the chemical components such as lignin and polysaccharides, whose chemical structure can be changed by oxidative and/or enzymatic reactions. Therefore, further investigations need to be performed to determine the optimal conditions for measurements as well as suitable data treatments to account for the spectral variations caused by aging, in order to be able to distinguish between *P. densiflora* and *P. thunbergii* on the basis of the differences in their spectra.

## Conclusions

When using unaging heartwood samples, we were able to identify *P. densiflora* and *P. thunbergii* by employing NIR

spectroscopy in combination with multivariate analysis. However, when aging wood samples were used, the proposed method was ineffective in distinguishing between the two species. Thus, the method is not suitable for classifying wood samples from historical and archeological buildings. However, further research is underway to find the spectral features between these microscopically similar species more significant than those caused by aging.

**Acknowledgments** The study was supported in parts by Grants-in-Aid for Scientific Research (Grant Numbers 25252033, 22300309, and 24780169) from the Japan Society for the Promotion of Science (JSPS). The authors thank Ms. Izumi Kanai and Mr. Akio Adachi for their technical support.

## References

- Schimleck LR, Evans R, Ilic J, Matheson AC (2002) Estimation of wood stiffness of increment cores by near-infrared spectroscopy. *Can J For Res* 32:129–135
- Adedipe OE, Dawson-Andoh B, Slahor J, Osborn L (2008) Classification of red oak (*Quercus rubra*) and white oak (*Quercus alba*) wood using a near infrared spectrometer and soft independent modelling of class analogies. *J Near Infrared Spectrosc* 16:49–57
- Gierlinger N, Schwanninger M, Wimmer R (2004) Characteristics and classification of Fourier-transform near infrared spectra of the heartwood of different larch species (*Larix* sp.). *J Near Infrared Spectrosc* 12:113–119
- Jones PD, Schimleck LR, Peter GF, Daniels RF, Clark A (2006) Nondestructive estimation of wood chemical composition of sections of radial wood strips by diffuse reflectance near infrared spectroscopy. *Wood Sci Technol* 40:709–720
- Horikawa Y, Imai T, Takada R, Watanabe T, Takabe K, Kobayashi Y, Sugiyama J (2012) Chemometric analysis with near-infrared spectroscopy for chemically pretreated *Erianthus* toward efficient bioethanol production. *Appl Biochem Biotechnol* 166:711–721
- Leinonen A, Harju AM, Venalainen M, Saranpaa P, Laakso T (2008) FT-NIR spectroscopy in predicting the decay resistance related characteristics of solid scots pine (*Pinus sylvestris* L.) heartwood. *Holzforschung* 62:284–288
- Hauksson JB, Bergqvist G, Bergsten U, Sjoström M, Edlund U (2001) Prediction of basic wood properties for Norway spruce. Interpretation of near infrared spectroscopy data using partial least squares regression. *Wood Sci Technol* 35:475–485
- Inagaki T, Schwanninger M, Kato R, Kurata Y, Thanapase W, Puthson P, Tsuchikawa S (2010) *Eucalyptus camaldulensis* density and fiber length estimated by near-infrared spectroscopy. *Wood Sci Technol* 46:143–155
- Schimleck LR, Jones RD, Peter GF, Daniels RF, Clark A (2004) Nondestructive estimation of tracheid length from sections of radial wood strips by near infrared spectroscopy. *Holzforschung* 58:375–381
- Schimleck LR, Evans R, Jones PD, Daniels RF, Peter GF, Clark A (2005) Estimation of microfibril angle and stiffness by near infrared spectroscopy using sample sets having limited wood density variation. *IAWA J* 26:175–187
- Schimleck LR, Michell AJ, Vinden P (1996) Eucalypt wood classification by NIR spectroscopy and principal components analysis. *Appita J* 49:319–324
- Braga JWB, Pastore TCM, Coradin VTR, Camargos JAA, da Silva AR (2011) The use of near infrared spectroscopy to identify

- solid wood specimens of *Swietenia Macrophylla* (Cites Appendix II). IAWA J 32:285–296
13. Pastore TCM, Braga JWB, Coradin VTR, Magalhaes WLE, Okino EYA, Camargos JAA, de Muniz GIB, Bressan OA, Davrieux F (2011) Near infrared spectroscopy (NIRS) as a potential tool for monitoring trade of similar woods: discrimination of true mahogany, cedar, andiroba, and curupixa. *Holzforschung* 65:73–80
  14. Sandberg K, Sterley M (2009) Separating Norway spruce heartwood and sapwood in dried condition with near-infrared spectroscopy and multivariate data analysis. *Eur J For Res* 128:475–481
  15. Watanabe K, Abe H, Kataoka Y, Nodhito S (2011) Species separation of aging and degraded solid wood using near infrared spectroscopy. *Jpn J Histor Bot* 19:117–124
  16. Mizuno S, Sugiyama J (2011) Wood identification of building components of Syue-do, Chion-in temple designated as nationally important cultural property. *J Soc Architect Hits Japan* 56:124–135
  17. Horikawa Y, Imai T, Takada R, Watanabe T, Takabe K, Kobayashi Y, Sugiyama J (2011) Near-infrared chemometric approach to exhaustive analysis of rice straw pretreated for bioethanol conversion. *Appl Biochem Biotechnol* 164:194–203
  18. Savitzky A, Golay MJE (1964) Smoothing and differentiation of data by simplified least squares procedures. *Anal Chem* 36:1627–1639
  19. Tsuchikawa S, Siesler HW (2003) Near-infrared spectroscopic monitoring of the diffusion process of deuterium-labeled molecules in wood. Part I: softwood. *Appl Spectrosc* 57:667–674
  20. Tsuchikawa S, Siesler HW (2003) Near-infrared spectroscopic monitoring of the diffusion process of deuterium-labeled molecules in wood. Part II: hardwood. *Appl Spectrosc* 57:675–681
  21. Watanabe A, Morita S, Ozaki Y (2006) A study on water adsorption onto microcrystalline cellulose by near-infrared spectroscopy with two-dimensional correlation spectroscopy and principal component analysis. *Appl Spectrosc* 60:1054–1061
  22. Tsuchikawa S, Yonenobu H, Siesler HW (2005) Near-infrared spectroscopic observation of the ageing process in archaeological wood using a deuterium exchange method. *Analyst* 130:379–384
  23. Yokoyama M, Gril J, Matsuo M, Yano H, Sugiyama J, Clair B, Kubodera S, Mitsutani T, Sakamoto M, Ozaki H, Imamura M, Kawai S (2009) Mechanical characteristics of aged Hinoki wood from Japanese historical buildings. *C R Physique* 10:601–611
  24. Siesler HW, Ozaki Y, Kawata S, Heise HW (2002) Near-infrared spectroscopy, principal instruments applications. Wiley, Weinheim